Dynamic Optimization of Evacuation Route in the Fire Scenarios of Offshore Drilling Platforms

Yanfu Wang[1, 2], Tao Wang[1], Weikai Ma[1], Fei Li[1], Xinjian Wang[3], Malkeson Sean[2], Zaili Yang[2], Jin Wang[2]

[1] College of Mechanical and Electronic Engineering, China University of Petroleum, Qingdao 266580, P.R. China

[2] Liverpool Logistics, Offshore and Marine (LOOM) Research Institute, Liverpool John Moores University, L3 3AF, UK

[3] Navigation College, Dalian Maritime University, Dalian 116026, P.R. China

Abstract: When fire occurs in an offshore platform, evacuation plays a vital role in safeguarding the evacuees' lives. How to efficiently evacuate to minimize the loss of life is a dynamic problem, requiring a continuing research effort with changing technologies. In this research, a dynamic optimization model is proposed to determine the optimized evacuation route in the fire scenarios of offshore platforms. Firstly, the road network model of an offshore platform is built in a Geographic Information System (GIS) environment based on the data from a real drilling platform. Secondly, drilling platform fires are simulated using Fire Dynamics Simulation (FDS), and then the fire simulation data is input into the proposed road network model. Thirdly, the traditional Ant Colony Optimization (ACO) Algorithm is improved by considering the influence of fire on evacuation to study the impact of high temperature, smoke and toxic gases on evacuation. Next, the improved route optimization algorithm and a road network model of the offshore platform are integrated to formulate a dynamic route optimization model for evacuation in fire scenarios. Finally, a case study is conducted to demonstrate the model on a drilling platform of Nan Hai in China. The results reveal that the equipment area around the fire source on the lower deck is mostly affected by the smoke. It is validated that the proposed model can be used to optimize the evacuation route to guide evacuees avoid the hazardous area according to the dynamic spread of smoke. This study can provide fast real-time guidance for the trapped evacuees during the evacuation process on offshore platforms by considering the influence of fire on evacuation.

Keywords: Offshore platform; Fire simulation; Geographic Information System; Optimal evacuation route; Dynamic optimization

1. Introduction

Accidents such as the Piper Alpha and Deepwater Horizon tragedies have been stimulating fire and evacuation research on offshore platforms. Once the fire occurs, it is often difficult for evacuees to evacuate from the extremely dangerous environment [1], and it is evident that most of the casualties occur during evacuation [2]. Therefore, it is important to study how to evacuate effectively and reduce the casualties during the evacuation on offshore platforms.

Previous research has been conducted on emergency evacuation on offshore platforms. These studies mainly focus on the following three aspects. Firstly, the evacuation on offshore platforms was investigated using risk assessment methods. For example, a risk assessment model was developed for escape and evacuation systems in harsh environmental conditions [3] and a methodology was introduced for identifying critical human and organizational factors in the escape, evacuation and rescue systems of offshore installations [4, 5]. Secondly, computer technology has

been used to simulate the emergency evacuation on offshore platforms [6, 7]. The research in this field is mainly divided into two categories: the evacuation simulation using some commercial software, such as Fire Dynamics Simulator with Evacuation（FDS+EVAC）, Pathfinder, STEPS, Building Exodus, and the development of new evacuation models [8]. Thirdly, models have been proposed for buildings and other public places [9, 10]. Comparatively, there are very few previous studies about evacuation route optimization on offshore drilling platforms, which have unique features in terms of fire and evacuation. Furthermore, a limited number of studies have investigated the effect of smoke on dynamic adjustment of evacuation routes in offshore platforms. Given the risk contribution on offshore platforms, overlooking the impact of smoke spreading on the evacuation will lead to significant gaps between theoretical studies and practical scenarios.

Soft computing techniques including artificial neural networks (ANN), support vector regression (SVR) and fuzzy logic (FL), are becoming more and more popular in solving real-life problems. For example, ANN becomes a research hotspot emerging in the field of artificial intelligence [11]. Based on ANN, Taormina used the Lower Upper Bound Estimation method and Multi-Objective Fully Informed Particle Swarm optimization algorithm to predict the streamflow discharges of rivers [12].

Computational Intelligence methods including computational intelligence (CI) and machine learning techniques, have become a significant tool in production and optimization of renewable energies [13]. It is highlighted that some computing techniques are used in exploring the evacuation optimization in emergency situations, such as, the Bayesian Network, Particle Swarm Optimization (PSO). Some algorithms like the Dijkstra, Floyd, A* algorithm and Ant Colony Optimization (ACO) have become more and more popular. Among them, ACO has the advantages of having a distributed parallel mechanism, strong adaptability and easy combination with other algorithms. However, the traditional ACO cannot be used to study the dynamic impact of fire on the routes. Therefore, it is modified to consider the real-time impact of fire, which can be used to adjust the optimal route dynamically according to the spread of smoke. The paper is organized as follows. In Section 2, FDS, ACO and their applications in fire and evacuation are reviewed. The concept of equivalent length is integrated with the road network model to study the influence of smoke spreading on evacuation in Section 3, and the influences of smoke temperature, visibility and carbon monoxide (CO) concentration are taken into account to determine the optimal evacuation route in fire scenarios. The methodology and its new features are demonstrated in a real case study in Section 4 before the conclusion in Section 5.

2. Literature review

2.1 Applications of FDS for evacuation in fire scenarios

There are some reported research findings on fire or evacuation separately. Recently, researchers have also studied the evacuation in fire scenarios. It is impossible to carry out any experiments invovling evacuees in any burning buidling, thus, computational tools, like fire models tend to be the best choice [14]. FDS is a field model-based software tool for computational fluid dynamics developed by the National Institute of Standards and Technology (NIST) [15, 16]. It has been widely used in the field of fire studies and has been verified and improved by a large number of experiments [17, 18].

FDS has often been integrated with evacuation models to study the evacuation in fire scenarios. EVAC is an evacuation module based on the social force model integrated in FDS, which can be used to simulate the development of fire and the evacuation simultaneously in the fire scenarios. FDS+EVAC

was often used to quantify the evacuation process and evacuation efficiency [18-20] or be compared with evacuation experiments [21-23]. Building Information Modelling (BIM) has been explored and integrated with FDS to evaluate the evacuation in case of fire [14, 24, 25]. Evacuation software tools such as STEPS [26], Pathfinder [27] and SIMULEX [28] have also been combined with FDS to study the changes of critical factors in fire scenarios and analyze the process of evacuation affected by these factors.

2.2 Applications of ACO for the optimization of evacuation route

ACO was proposed initially to solve the Traveling Salesman Problem and has been widely used in route optimization. To solve the problem of dynamic change of information and continuous uncertainty in the disasters, Yi [29] used ACO to solve the logistics problem arising in disaster relief activities and proved the effectiveness of the method. Fang [30] improved the ACO to achieve the goals of minimizing the total evacuation time. Considering the distance to the target area, the length of waiting area and queue length, Yang [31] used ACO to predict the queue distribution of the evacuation process and simulated the evacuation process using FDS+EVAC to verify the accuracy of the predicted results.

While the previous studies focused on minimizing evacuation distance, they failed to take into account the dynamic impact of fire (*i.e.* smoke spreading) on evacuation. In this paper, FDS and ACO are integrated for the first time to develop an improved route optimisation algorithm enabling the optimal evacuation routing considering the real time impact of fires on offshore drilling platforms.

3. Methodology

The methodology of developing a new evacuation model is outlined in this section. The steps are detailed in the ensuing sections. Firstly, the road network model of an offshore platform is established using ArcGIS. ArcGIS is used for compiling geographic data, analyzing mapped information and managing geographic information in a database. Secondly, FDS is used to simulate the offshore platform fire and then the simulation data is incorporated into the proposed road network model. Thirdly, the traditional ACO is improved and applied in the offshore platform fire evacuation by taking into account the dynamic impact of fire.

3.1 Dynamic evacuation route optimisation model

At present, the most widely used GIS series software in the world is ArcGIS, which has a world market share of more than 85% with relatively perfect functions and stable performance. ArcGIS has the advantages of spatiotemporal data management, spatial query and analysis functions. Furthermore, it can be combined with computer simulation technology to study the evacuation of evacuees in the building. Therefore, ArcGIS is adopted to establish the road network model of an offshore platform in this section. The evacuation route optimisation model for the fire scenarios of offshore platforms is developed using VS2010 and ArcGIS as shown in Fig.1, which includes four parts. Part1 includes a common function of a GIS map, such as zooming in and out of the map. Part2 is used to display the spreading of smoke and the real-time route optimisation results, which provides a visualized disaster situation for the emergency decision makers. The red colour indicates impassable routes (level 1), the orange colour indicates higher danger at level 2, the yellow colour reveals lower danger at level 3 and the black colour means safe (level 4). In Part3, when the starting and ending points are set up, the optimal evacuation route, the equivalent length of route and the required safe egress time can be determined. Part4 can be used to display the layer and classification information relating to the current road network.

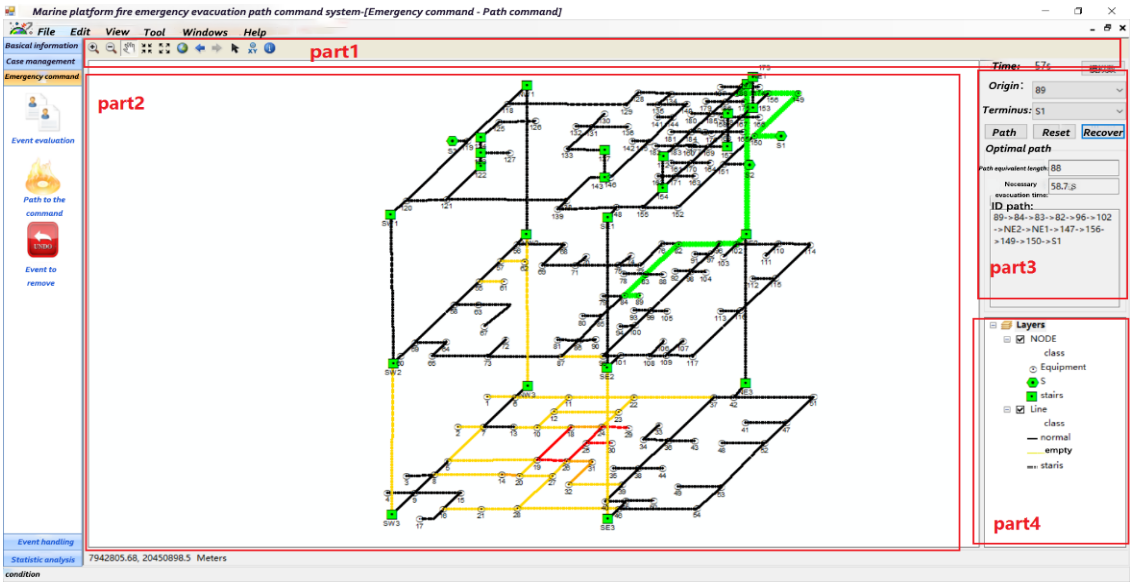

Fig.1 Evacuation route optimisation system

3.2 Fire simulation of offshore platforms

In this section, FDS software is adopted to establish the physical model of an offshore drilling platform (*e.g.*, one in Nan Hai China). The software solves numerically a form of the Navier-Stokes equations appropriate for low-speed, thermally driven flows, with an emphasis on smoke and heat transportation from fires. The thermal properties of the surface materials are defined and the internal structural features are simplified to form a simplified physical model as shown in Fig.2.

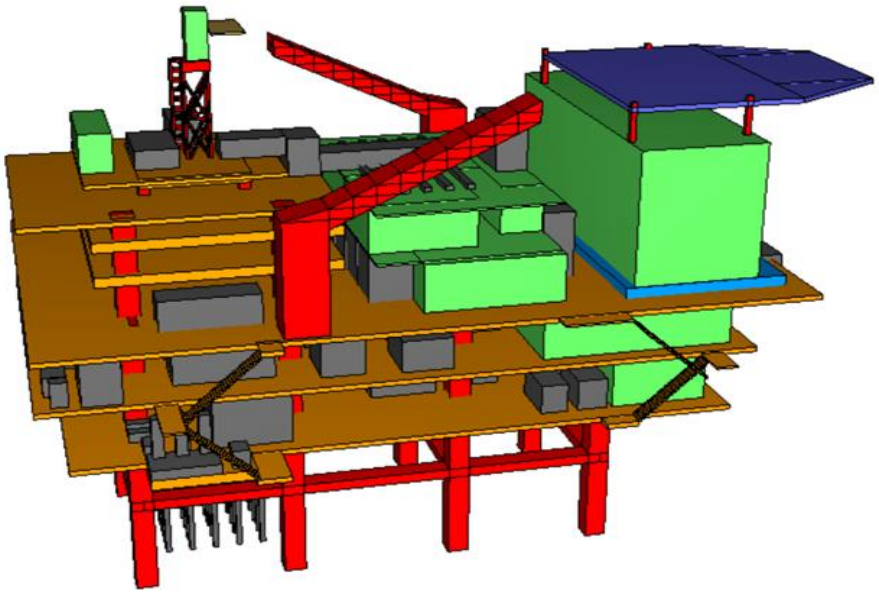

Fig.2 Physical model of an offshore platform

For simulations involving buoyant plumes, a measure of how well the flow field is resolved given by the non-dimensional expression D^*/δ_x [32].

$$\mathrm{D}^* = \left(\frac{\dot{\mathrm{Q}}}{\rho_\infty \mathrm{c_p} \mathrm{T}_\infty \sqrt{\mathrm{g}}}\right)^{\frac{2}{5}} \tag{1}$$

$$4 \le \frac{\mathrm{D}^*}{\delta_x} \le 16 \tag{2}$$

where, D^* is the characteristic diameter of the fire source (m), δ_x is the nominal size of a mesh

cell (m), $\dot{Q}$ is the total heat release rate of the fire source (kW), ρ_∞ is the air density (kg/m^3), c_p is the thermal capacity of air (J/K), T_∞ is the ambient air temperature (K) and g is gravitational acceleration (m/s^2).

The quantity D^*/δ_x can be considered as the number of computational cells spanning the characteristic diameter of the fire, which should range between 4 and 16 according to the validation study sponsored by the U.S. Nuclear Regulatory Commission [33]. To ensure that D^*/δ_x varies from 4 to 16, δ_x should range from 0.2 to 0.8m. Therefore, a relatively coarse mesh (0.8 m × 0.8 m × 0.8 m) was built firstly, and then gradually refined until no appreciable differences can be seen from the results. Based on the mesh independent tests, the mesh around the oil pool is determined as 0.25 m × 0.25 m × 0.25 m and in the remaining part 0.5 m × 0.5 m × 0.5 m.

The computational domain refers to an external volumetric region that surrounds the offshore platform model, where the basic flow equations are solved. A key factor that influences the accuracy and computational expense of FDS simulations is the size of the computational domain. The effect of the computational domain on FDS simulation results is investigated with a series of sensitivity studies.

Thermocouples are designed in the downwind direction to record the temperature data for different computational domains. As shown in Fig.3, the thermocouples are set on the south side of the platform considering the north wind is the dominant wind direction all year round.

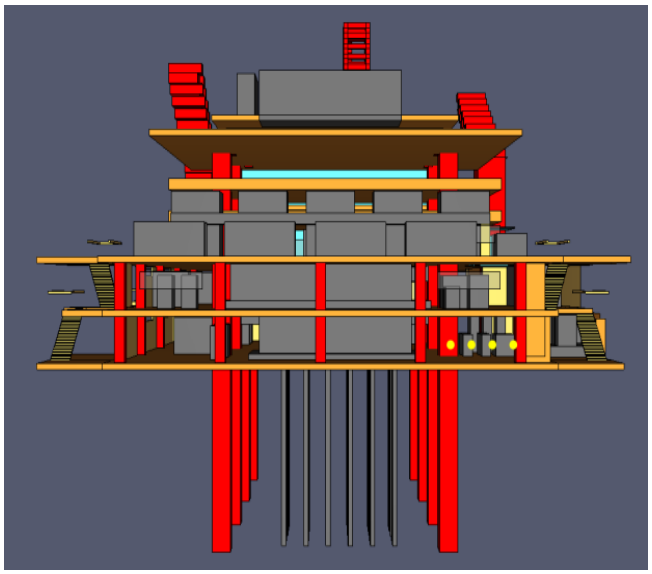

Fig.3 Schematic diagram of thermocouples arrangement

Different computational domains, such as twice/ 3-times/ 4-times/ 5-times/ 6-times the height of the platform are considered here. The temperature profiles with different domain heights are shown in Fig.4 (a). It can be observed that the distribution of temperature for twice, 3-times and 4-times the height of the platform has a large gap with 5-times and 6-times. Therefore, 5-times the height of the platform is selected for further study to be the suitable computational domain in Z direction.

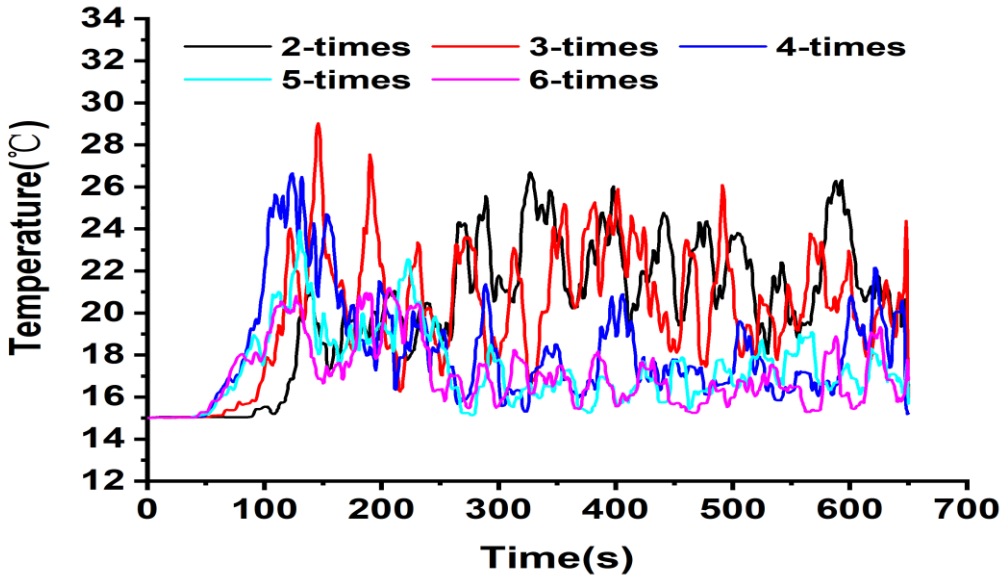

(a) Z direction

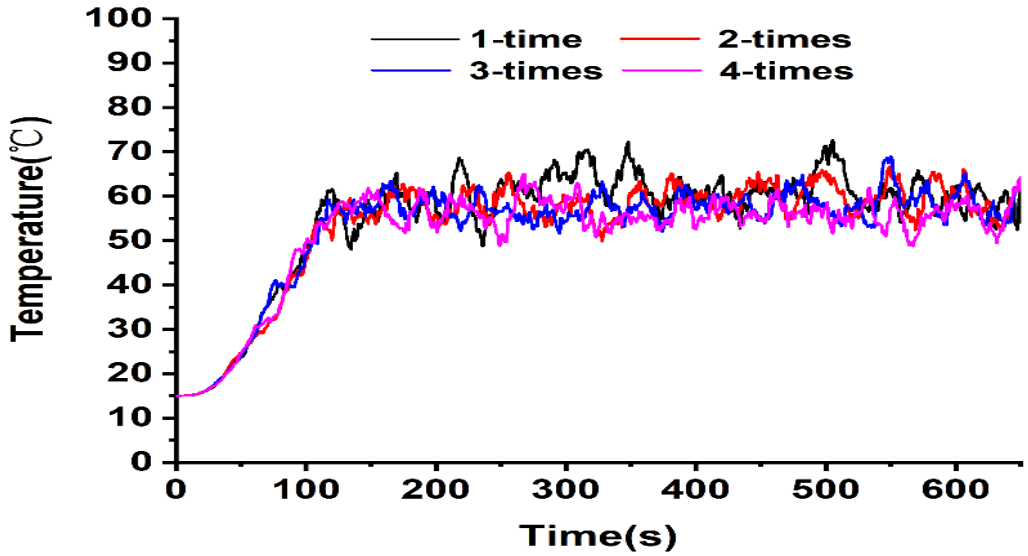

(b) Y direction

Fig.4 Temperature for different simulation domains

Computational domains with 1-time/ twice/ 3-times/ 4-times the width of the platform are compared. The temperatures for different computational domains in Y direction are shown in Fig.3 (b). From Fig.3 (b), the distribution of temperature for 1-time the width of the platform has a large gap when compared with twice/ 3-times/ 4-times the width of the platform. Therefore, twice the width of the platform is determined in Y direction. In summary, 5-times the height and twice the width of the platform are selected to be the suitable computational domain in Z and Y directions.

For the boundary conditions, ambient temperature is 15℃ and the relative humidity is 60%. The surface type of all the mesh boundary is defined as “Open”. The simulation time is set 650s. The properties of the materials used in the case study are shown in Table 1 [32, 34-36].

Table 1. Properties of the materials used in the simulation model

	Concrete	Steel	Crude oil
Emissivity [-]	0.85	0.80	0.85
Density [kg/m^3]	2300	7850	830-880
Specific heat capacity [kJ/kg·K]	1.05	0.60	2
Heat conductivity [W/m·K]	1.40	45	0.14
Heat of combustion [kJ/kg]	-	-	42.6

Based on the statistical analysis of fire accidents in the Gulf of Mexico reported by the Bureau of Safety and Environmental Enforcement [37], the fire scenario with the highest frequency is that the crude oil in the pipeline leaks in the equipment area of the lower-deck, causing pool fire. Because the fire development growth rate of oil pool fire belongs to the ultrafast fire of the t^2 fire model, the t^2 fire model is adopted here to effectively describe the characteristics of the oil pool fire [38]. In the t^2 fire model, the heat release rate is assumed to be proportional to the square of the burning time:

$$Q(t) = \alpha t^2$$

where:

Q = the heat release rate of the fire at any time (kW); and

α = the coefficient for t^2 fire is fuel dependent, 0.1876 (kW/s^2).

The value of α can be selected according to Table 2.

Table 2. The value of α

Description	Value of α (kW/s^2)
Slow	0.00293
Medium	0.01172
Fast	0.0469
Ultrafast	0.1876

High-temperature smoke may cause panic and reduce the judgment ability of evacuees. According to the relevant literatures [39], temperature [40], visibility [41] and CO concentration [42] are defined as the key risk indexes. The hazards of various factors are divided into 4 levels [39] and the critical values are determined as shown in Table 3, which is used to define the status of the evacuation route.

Table 3. Hazard Classification of Influential Factors

Hazardous factors	Safe	Dangerous	More Dangerous	Extremely Dangerous	Critical value
	Level 4	Level 3	Level 2	(Causing death) Level 1	
Temperature/℃	<42	42~65	65~100	>100	65
Visibility/m	>20	5~20	1~5	<1	5
CO/%	<0.08	0.08~0.16	0.16~0.32	>0.32	0.16%

3.3 Evacuation route optimisation algorithm

The fire spreads rapidly on offshore platforms because there are many ignitable materials. With the spreading of smoke, some evacuation routes are not accessible. In this section, an improved ACO is developed to supply guidance for personnel to evacuate according to the dynamic spreading of smoke.

In the equation,

$allowed_k$: Location nodes to be visited by ant k positioned on point i;

$\tau_{ij}(t)$: Pheromone concentration between two points;

$\eta_{ij}(t)$: Heuristic factor, which stands for the visibility of the edge (i, j) between two points;

d_{ij} : Distance between two points, m;

α: Relative importance of pheromone concentration $\tau_{ij}(t)$; and

β: Relative importance of heuristic factor $\eta_{ij}(t)$.

Pheromone on the route will be updated. The route selected by the ant who found the feeding source is compared with the existing optimal route. If the new route is better than the old one, the optimal route will be updated, and the pheromone on the new route will be updated according to the pheromone update rule. When all ants complete a search, the pheromone concentration on each route is adjusted according to the following equation.

(3) Termination criteria: If the maximum number of iterations has been reached, the algorithm terminates and the optimal route is obtained.

3.3.1 Improved ACO for Fire Scenarios

The traditional ACO cannot reflect the influence of smoke. In the fire scenarios, the available route of an offshore platform varies with time under the influence of fire. Hence, it is necessary to improve the traditional ACO to characterize the dynamic influence of fire.

Because an offshore drilling platform has the characteristics of intensive equipment, numerous cabins, limited area and narrow escape route, it is difficult for evacuees to evacuate fast. When one chooses the route in the fire scenarios of an offshore platform, he/she should consider not only the actual length of the route but also the influence of smoke. There are two-categories of relevant influential factors. One is the route-related influential factors, including the width, passable state and the type (horizontal escape route and stairway, *etc*.) of the route, which are known before the occurrence of fire. The other is smoke-related influential factors, which are closely associated with the dynamic propagation of smoke, including temperature, visibility and CO concentration.

From the state transition probability equation of the ACO, it can be deduced that visibility η_{ij} is equal to $\frac{1}{d_{ij}}$, where d_{ij} is the linear distance between the nodes i and j. Obviously, it is unreasonable to use a linear distance directly to calculate the state transition probability in the fire scenario, thus, it is necessary to improve the calculation equation of linear distances when taking into account the real-time influence of smoke.

In this research, the concept of equivalent length is incorporated into the state transition probability equation to characterize the influence of the above two types of factors on the evacuation. W_{ij} represents the equivalent length of the route between nodes i and j. W_{ij} is calculated as follows:

$$W_{ij} = \left(k_{gij}\, k_{vij}\right) d_{ij} \tag{3}$$

where,

W_{ij} : the equivalent length of route, m;

k_{gij} : the route influential coefficient;

k_{vij} : the smoke influential coefficient; and

d_{ij} : the actual length of the route, m.

The route influential coefficient is calculated as follows [43].

$$k_{gij} = \frac{Mgv_0 sin\theta_{ij}}{P_0} + \cos\theta_{ij} \tag{4}$$

where,

M: the mass of the human body (M = 80kg in the case of a male adult);

g: the acceleration of gravity, m / s^2;

v_0 is the normal velocity, m/s (v_0=1.2m/s in the case of a male adult);

θ_{ij}: Angle of inclination, degree; and

P_0: Mobility (P_0 = 200 W in the case of a male adult), W;

The smoke influential coefficient is calculated as follows [42, 44].

$$k_{vij} = (1 + L_r + w_{co} + L_T) \tag{5}$$

where,

L_T: The temperature influential coefficient;

L_r : The visibility influential coefficient; and

w_{co}: The toxicity influential coefficient.

The influence of temperature on the evacuation velocity in the fire scenarios was studied through a series of experiments and deduced the equation for calculating the temperature influential factors [45]:

$$f_1(\mathrm{T}) = \begin{cases} 1, & T_s \le 40℃ \\ \dfrac{(v_{max} - 1.2)\left(\dfrac{T_s - T_{c1}}{T_{c2} - T_{c1}}\right)^2}{1.2} + 1, & 40℃ < T_s \le 65℃ \\ \dfrac{v_{max}}{1.2}\left[1 - \left(\dfrac{T_s - T_{c2}}{T_{dead} - T_{c2}}\right)^2\right], & 65℃ < T_s \le 100℃ \\ 0, & T_s > 100℃ \end{cases} \tag{6}$$

where,

v_{max}: The max movement speed of evacuee, m/s;

T_s: Environment temperature, ℃;

T_{c1}: Temperature at which evacuee feel uncomfortable, ℃.;

T_{c2}: Temperature at which evacuee are injured, ℃; and

T_{dead}: Temperature at which evacuee are dead, ℃.

The temperature influential coefficient is $L_T = \frac{1}{f_1(\mathrm{T})} - 1$.

To study the influence of visibility, a number of experiments were carried out [45] and the equation of the visibility influential factor was deduced as follows [46]:

$$f_2(\mathrm{k}) = \begin{cases} 1 & k \ge 20 \\ -0.618k^{-0.26} & 1 \le k < 20 \\ 0.1 & k < 1 \end{cases} \tag{7}$$

where，k: visibility, m; and

Visibility influential coefficient $L_r = \frac{1}{f_2(\mathrm{k})} - 1$.

Smoke contains a large amount of toxic and harmful gases due to incomplete combustion, while the most dangerous component is carbon monoxide (CO). The influence of carbon monoxide concentration is characterize by the following equation [37, 44]:

$$f_3(\mathrm{c}) = \begin{cases} 1 & c \le 0.1 \\ 1 - (0.2125 + 1.788c) \cdot c \cdot t & 0.1 < c < 0.32 \\ 0 & c \ge 0.32 \end{cases} \tag{8}$$

The toxicity influential coefficient is $w_{co} = \frac{1}{f_3(\mathrm{c})} - 1$

where:

c: Carbon monoxide concentration (%); and

t : Exposure time of evacuee, s.

The total smoke influential coefficient is calculated using Eq.9.

$$k_{vij} = (1 + L_r + w_{co} + L_T) = (\frac{1}{f_1(\mathrm{T})} + \frac{1}{f_2(\mathrm{k})} + \frac{1}{f_3(\mathrm{c})} - 2) \tag{9}$$

The heuristic factor is obtained using Eq.10.

$$\eta_{ij} = \frac{1}{W_{ij}} = \frac{1}{(k_{gij}\, k_{vij})\, d_{ij}} \tag{10}$$

The transition probability is obtained using Eq.11.

$$P_{ij}^{k}(t) = \begin{cases} \dfrac{\tau_{ij}^{\alpha}(t)(\frac{1}{(k_{gij}\, k_{vij})\, d_{ij}})^{\beta}(t)}{\sum_{s \in allowed_k} \tau_{is}^{\alpha}(t)\eta_{is}^{\beta}(t)}, & \mathrm{j} \in allowed_k \\ 0, & \text{otherwise} \end{cases} \tag{11}$$

The optimal evacuation route between h and j (safety location) should satisfy the following objective function.

$$F = \begin{cases} 0 & (h = j) \\ min\, W_{hj} & (h \neq j) \end{cases} \tag{13}$$

3.3.2 Significance of Ant Colony Optimisation Parameters

The relevant parameter settings of ACO affect the final results directly. A reasonable parameter setting can not only improve the calculation efficiency, but also ensure the quality of the optimal solution. As there is no exact mathematical calculation formula for the relevant parameters of the ACO method available, some data is preliminarily set based on the literatures and a series of tests are carried out to analyze the influence of each parameter on the optimisation performance. In these sensitivity tests, based on the optimal parameter setting determined by Marco Dorigo's experiments [53], the initial values are set as: N = 90 (N is the number of ants), $\alpha = 1$ (α is the heuristic factor), $\beta = 2$ (β is the expected heuristic factor), $\rho = 0.3$ (ρ is the Pheromone volatilization factor), Q=1000 (Q is pheromone intensity) [47, 48]. Because the ACO method is a heuristic algorithm, the results have a certain degree of randomness, and multiple experiments should be carried out to reduce the error caused by this contingency. One parameter is changed in each group and the simulation is run for 10 times, then the average value is taken. The road network model of the offshore platform in Fig. 1 is taken as an example for testing, the same starting and ending points are defined for all the tests. The starting point (node 25) is the equipment area in the middle of the lower deck and the end point (node S1) is the lifeboat assembly area.

(1) Influence of ants' number (N) on the algorithm performance

Ants cooperate with each other to find the optimal route. The route selected by each ant is a sub-scheme of the feasible solution sets. The number of ants directly affects the quality of the optimal solution. Therefore, the global optimisation capability and stability of the algorithm can be improved by increasing the number of ants. However, when the number is too large, the pheromone concentration on the searched route will tend to be average, and the positive feedback effect will be weakened and the operating efficiency of the algorithm is therefore reduced. Oppositely, the number should not be too small; otherwise, it will reduce the search accuracy of the algorithm and the global optimisation ability. The influence of the ant number is shown in Fig.5.

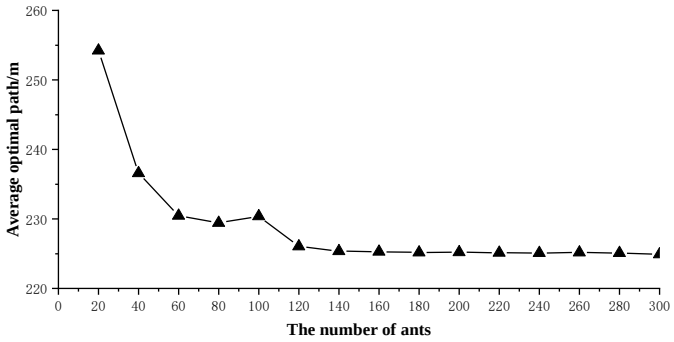

Fig.5 The effect of ant number on experimental results

From Fig. 5, it can be seen that when N < 120, the global optimisation ability of the algorithm is weak, and it is easy to fall into the local optimum. As the quantity of the ants continues to increase, the global optimisation ability of the algorithm is gradually improved with a marginal effect when N is over 160.

(2) The impact of α on algorithm performance

The heuristic factor α reflects the influence of the pheromone concentration on the route finding process. Normally, the larger α is, the more significant the influence of the pheromone on the route finding process. If α is too small, the positive feedback effect will be weakened, the sensitivity of ants to the pheromone on the route will be lower and the randomness of the route chosen by the ants will be increased, which will reduce the computational efficiency of the algorithm. The ants tend to choose a route with a higher pheromone concentration. The influence of the heuristic factor on the optimisation results is shown in Fig.6.

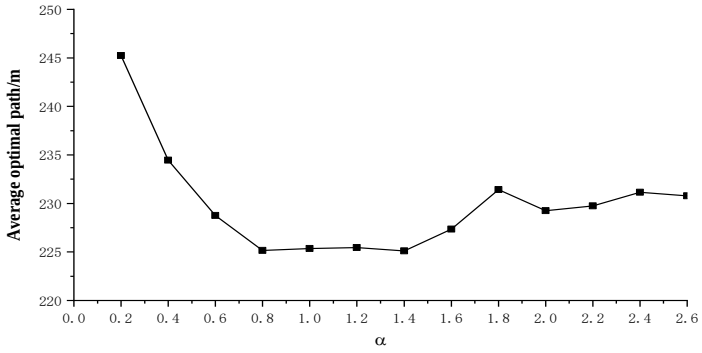

Fig.6 The effect of α on optimisation results

As Fig.6 shows, when α is less than 0.8, the positive feedback effect is weak, and the optimisation ability of the algorithm is not strong. When α is greater than 1.6, the positive feedback effect is enhanced. However, the possibility of stagnation or premature convergence increases, and it is easy to fall into a local optimum. Therefore, the value of [0.8, 1.4] is more rational for α.

(3) The impact of β on algorithm performance

β is the expected heuristic factor, which mainly reflects the guiding effect of route information on the optimisation process. It has important influence on the performance of ACO. The larger the β is, the more the ants are affected by the route information, and the higher possibility that the ants choose the local optimum. The influence of the expected heuristic factor is shown in Fig.7.

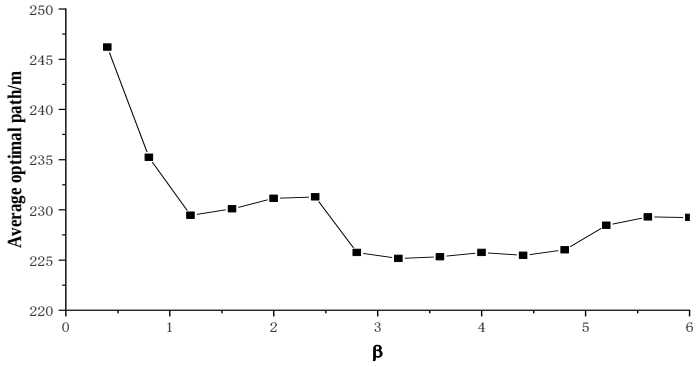

Fig.7 The effect of β on optimisation results

From Fig.7, it can be seen that the route information has a less influence on the ants, and the computational efficiency of the algorithm is reduced when β is small. When β is too large, the calculation efficiency is improved, but it is prone to premature phenomenon. Therefore, the value of [2.8, 4.8] is rational.

(4) The impact of ρ on algorithm performance

Pheromone volatilization factor ρ has a direct impact on the global search ability and convergence speed. If ρ is too small, the pheromone concentration on each route is similar, the positive feedback effect of information is lower. As a result, the calculation efficiency of the algorithm may be lower. Conversely, if ρ is too large, although the calculation efficiency can be improved, it reduces the algorithm's random searching ability and increases the possibility of the algorithm falling into a local optimum. The influence of the pheromone volatilization factor on optimisation results is shown in Fig.8.

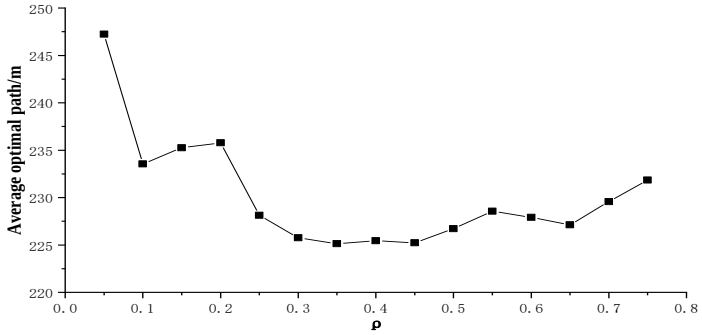

Fig.8 The effect of ρ on optimisation results

From Fig.8, when ρ is small, because the pheromone concentration difference of each route is not large, the ants have a certain degree of blindness when choosing a route, and it is easy to fall into a local optimum. When ρ is larger, the global search ability is improved, but the information interaction between ants is weakened. Therefore, the value of [0.3, 0.5] is appropriate for ρ.

(5) The impact of Q on algorithm performance

The pheromone intensity Q has important influence on the positive feedback performance. The larger the Q is, the faster the accumulation of pheromone. The positive feedback effect is therefore enhanced. However, if Q is too large, the global optimisation capability will reduce due to excessive positive feedback. The influence of the pheromone intensity Q on the optimisation results is shown in Fig.9.

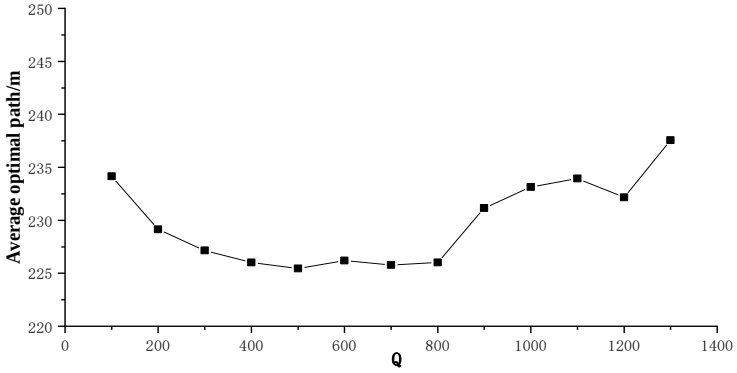

Fig.9 The effect of **Q** on optimisation results

From Fig.9, it can be seen that the calculation performance is unstable when Q is greater than 800. The value of [400, 800] is appropriate. In light of the above analysis, the optimal setting of the ACO parameters for the proposed road network model are summarized in Table 4.

Table 4. ACO parameter settings

Ants' number N	Heuristic factor α	Expected heuristic factor β	Pheromone volatilization factor ρ	Pheromone intensity Q
160	1.1	3.6	0.4	600

3.4 Validation of the proposed route optimization algorithm

In order to validate the proposed route optimization algorithm that can be used to dynamically adjust and optimize the routes according to the spread of fire smoke, the following case study is designed. Firstly, the road network model of the lower deck is taken. Secondly, the optimal route from the exit of the NW3 stairway to the SE3 stairway is found without fire. Then the fire smoke data is loaded to determine the optimal route between the two nodes at different times. The route optimization results are shown in Fig.10.

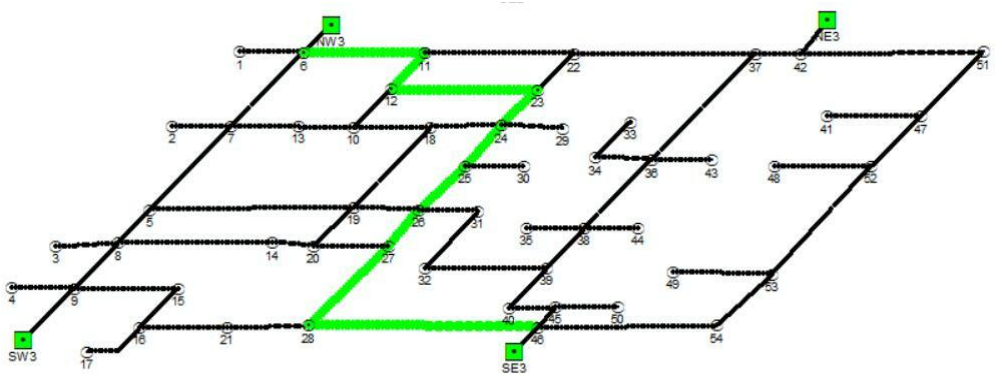

(a) Optimal evacuation route without considering the impact of fire

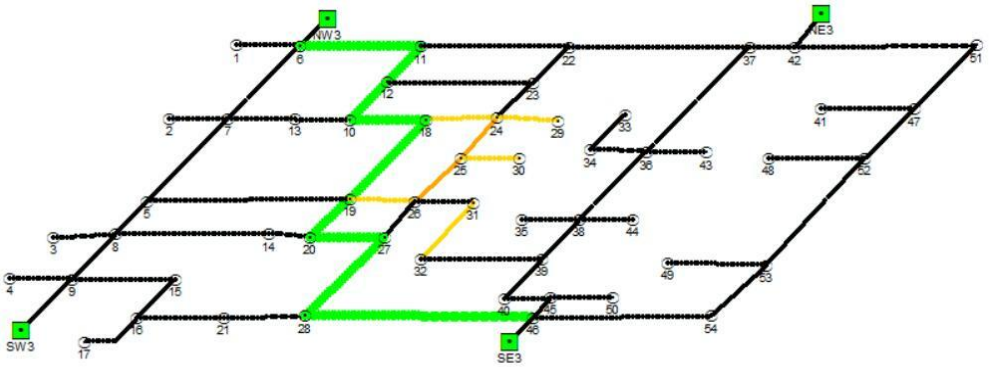

(b) Optimal evacuation route at 30s after the fire occurs

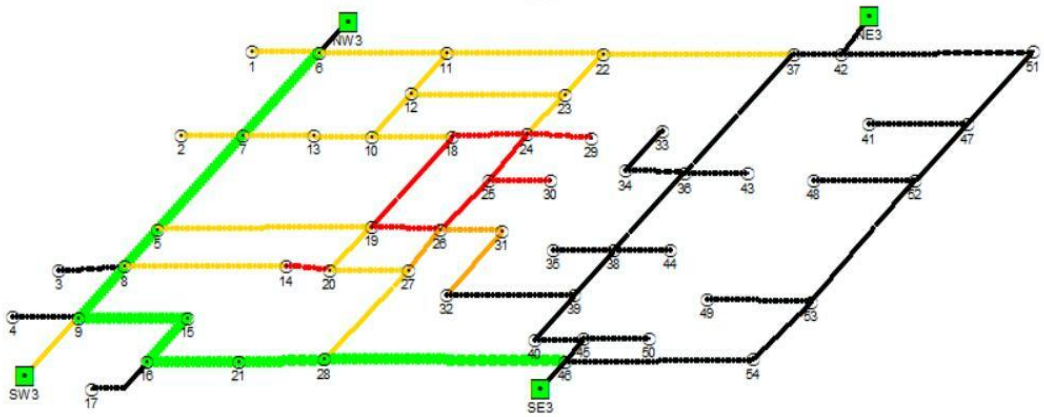

(c) Optimal evacuation route at 60s after the fire occurs

Fig.10 Verification of the proposed optimization algorithm

From Figure10(a), the optimal route from node 6 to node 46 is 6->11->12->23->24->25->26->27->28- >46 , its equivalent length is 75m without considering the influence of fire smoke. After the smoke data is loaded, the danger of route 24->26 is increased and the improved ant colony algorithm is used to re-plan the optimal route as shown in Figure 10 (b). The optimal route from node 6 to node 46 changes to 6->11->12->10->18->19->20->27->28->46, avoiding the dangerous route 24->26. Its equivalent length is 75m. As the fire spreads, some routes are unavailable. The route is optimized again at 60s after the fire occurs as shown in Figure 10(c). The optimal route from node 6 to node 46 changes to 6->7->5->8->9 ->15->16->21->28->46, the equivalent length becomes 98.4m. This validates the feasibility that the proposed route optimization algorithm can be used to consider the effects of smoke on evacuation routes.

4. A case study and result discussions

4.1 Road network of an offshore platform in Nan Hai China

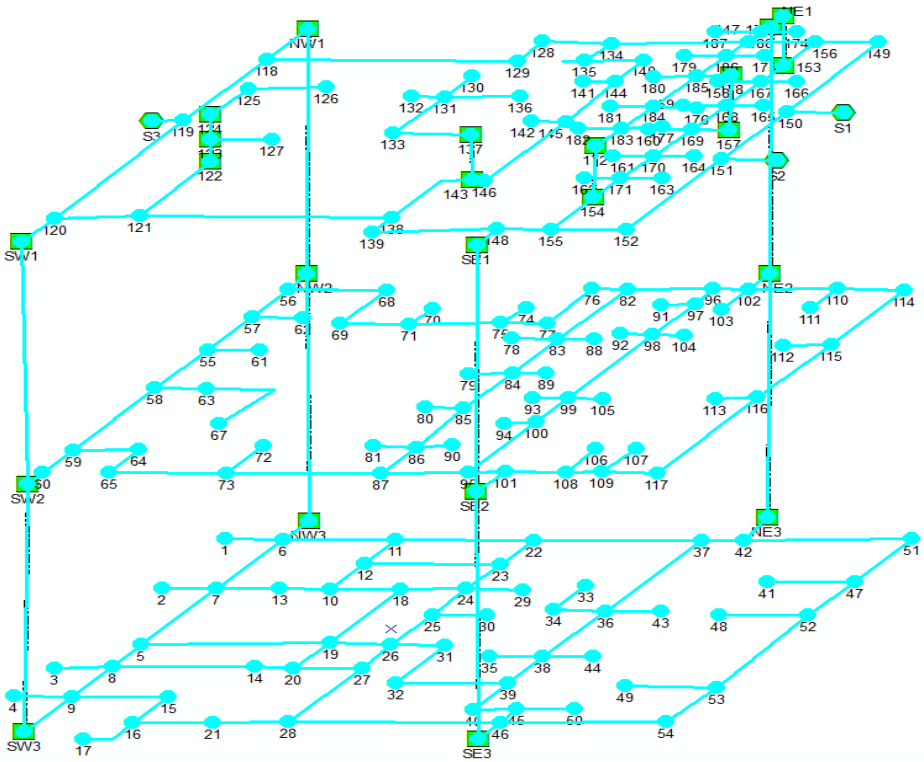

Fig.11 Road network of an offshore platform

In this section, the road network model of the offshore platform in Section 3.2 is established using the graph theory method. As shown in Fig.11, the model is mainly composed of nodes and routes. The key equipment points and the intersections of two routes are defined as nodes. The edge between two points represents the route.

4.2 Fire simulation

In this section, the t^2 fire model is adopted to effectively describe the development characteristics of fire. For the crude oil, the value of soot production should be set as 0.097, and the other fire source parameters are shown in Table 5 [41].

Table 5. Parameter settings of fire source

Diameter of leakage source, mm	Release rate, kg/s	Pool diameter, m	Pool area, m^2	Combustion mass loss rate, $kg/(m^2 \cdot s)$	Fire development time, s
50	24.5	4.62	21.34	0.098	323

4.2.1 Smoke propagation

The smoke propagation at different times after the start of a fire is shown in Fig.12.

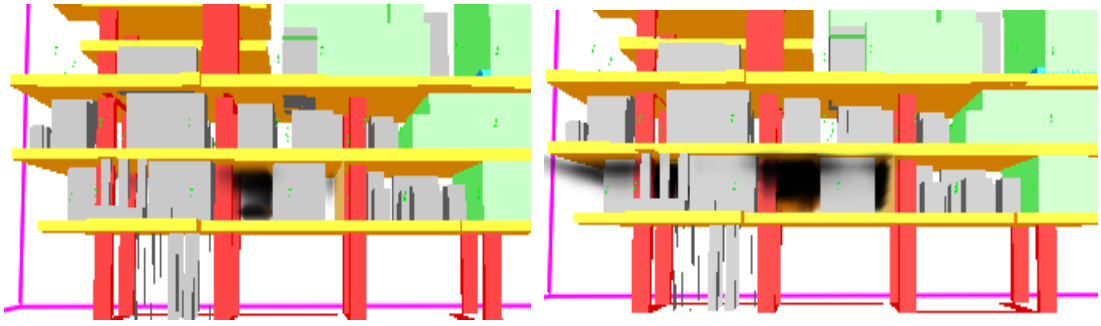

25s after the start of the fire

90s after the start of the fire

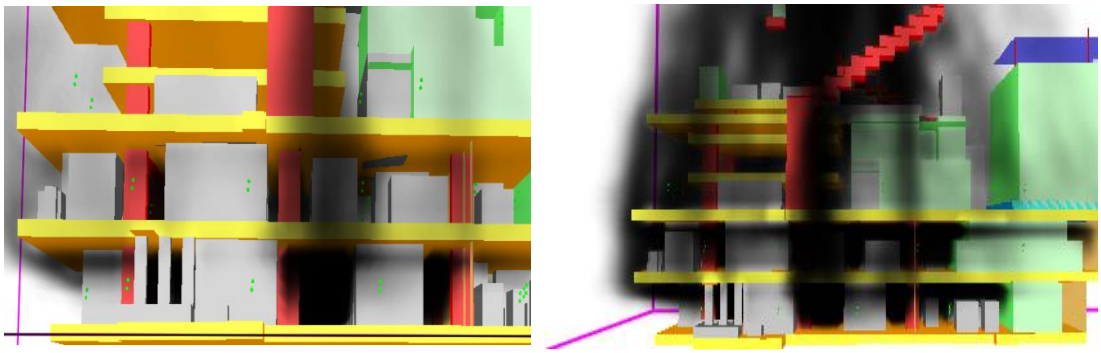

190s after the start of the fire　　600s after the start of the fire

Fig. 12 Smoke propagation of the offshore platform

It can be seen that the smoke begins to spread from the oil pipeline to nearby equipment on the lower deck after 25s. The rising smoke plume forms above the fire source. The high-temperature smoke gradually gathers under the mezzanine deck and begins to spread around. At approximately 90s, the smoke extends to the boundary of mezzanine deck and begins to spread to the other areas of mezzanine deck and upper deck. At 190s, the mezzanine deck is filled with smoke and some smoke also propagates to the area of the upper deck. Due to the blocking of the firewall, the cabins on the east area of the lower deck and mezzanine deck are less affected by the smoke during the early stage. However, with the spread of smoke, the cabins on the east area of the two decks were almost surrounded by smoke at 600s. Due to the blocking of the firewall, the living area located at the open area of the upper deck is less affected by smoke.

4.2.2 CO Concentration

In this section, the CO concentration around the stairways of the mezzanine deck and upper deck are shown in Fig.13. As shown in Fig.11, SW2 is the south west stairway of the mezzanine deck, NW2 is the north west stairway of the mezzanine deck, SE2 is the south east stairway of the mezzanine deck and NE2 is the north east stairway of the mezzanine deck. SW1 is the south west stairway of the upper deck, NW1 is the north west stairway of the upper deck, SE1 is the south east stairway of the upper deck and NE1 is the north east stairway of the upper deck.

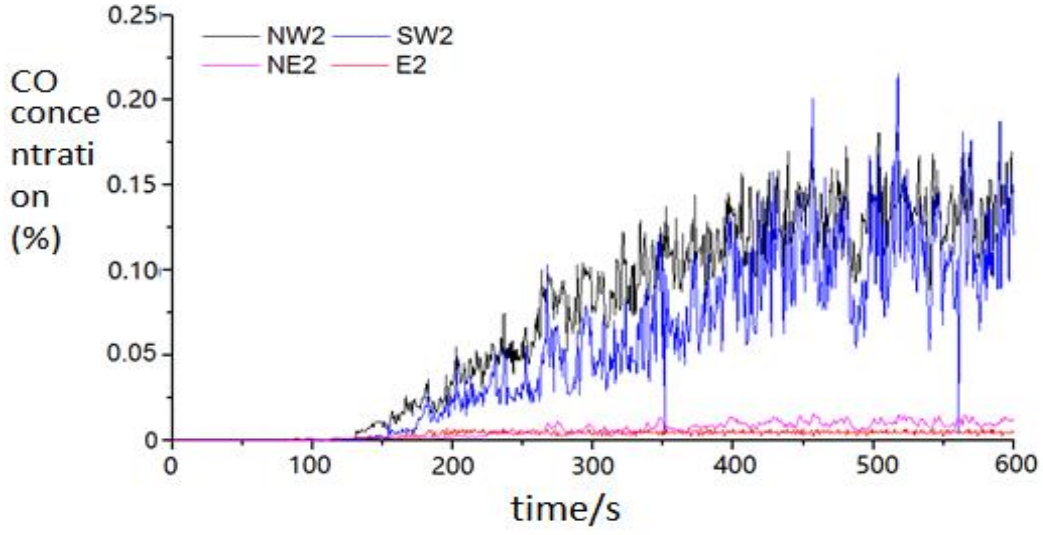

(a) CO concentration around each stairway on the mezzanine deck

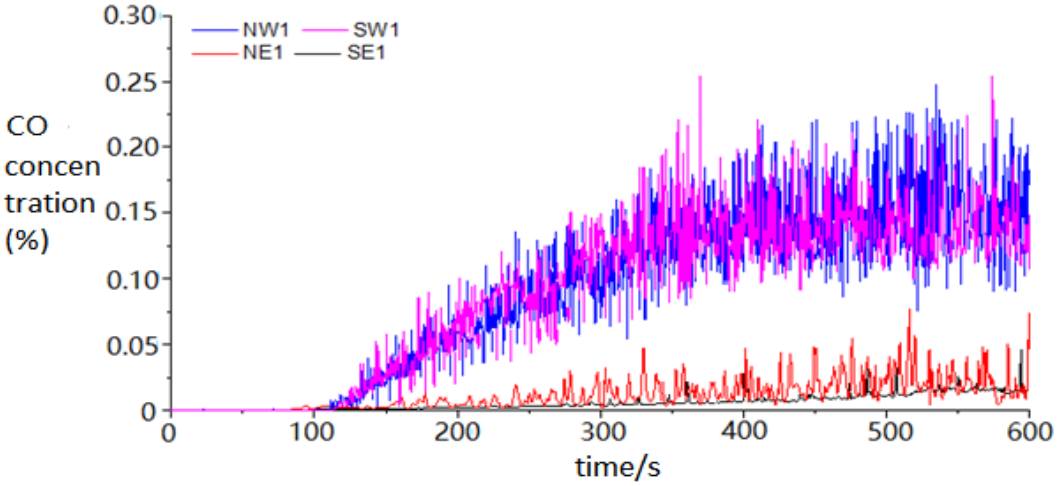

(b) CO concentration around each stairway on the upper deck

Fig.13 CO concentration around each stairway on the mezzanine deck and upper deck

From Fig.13, the CO concentration around the north west and south west stairways increases rapidly. During the stable stage of fire development, the CO concentration exceeds the critical value (0.16%). If the evacuees stay in this environment for a few minutes, they may become injured. The CO concentration around the north east and south east stairways is smaller than the north west and south west stairways.

4.3 Optimisation of evacuation route for fire scenarios

For the case study of the oil pool fire caused by the leakage of the oil pipeline at the lower deck of the offshore drilling platform, the influence of smoke spreading on the availability of the evacuation route is mainly analysed. Lifeboats are usually selected as the escape tool once fire occurs. The evacuation route to the muster station is investigated to obtain the optimal route at different times. The road network model of offshore platform is established using ArcGIS software. The influential functions and the equivalent length of each evacuation route are determined according to the maximum value (such as the maximum temperature, visibility and toxicity) along the evacuation routes. Then, the optimal evacuation route can be determined using the improved ACO method.

The optimal evacuation route from the chemical pharmacy area of the lower deck (node 27) to the muster station (S1) at different time (0s, 60s and 130s after fire occurs) is shown in Fig.14. The optimal evacuation route from the emergency power generation room of the mezzanine deck (node 93) to the muster station (S1) is shown in Fig.15 at different times (0s, 120s and 300s after fire occurs).

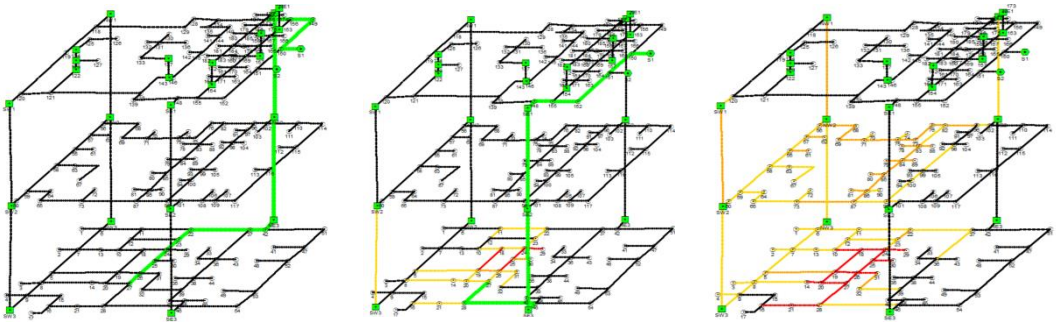

0s after fire occurs　　60s after fire occurs　　130s after fire occurs

Fig.14 The optimal evacuation route from the equipment area of lower deck to muster station in fire scenarios

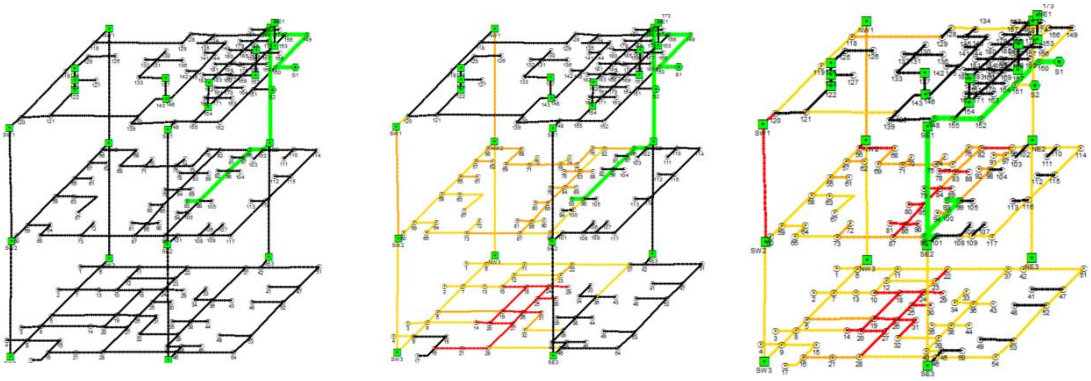

0s after fire occurs　　120s after fire occurs　　300s after fire occurs

Fig.15 The optimal evacuation route from the office area of mezzanine deck to muster station in fire scenarios

The detailed optimal evacuation routes at different times are summarized in Table 6.

Table 6. The optimal evacuation routes taking into account the influence of smoke

Starting point	Time/s	Optimum route to the muster station S1	Required safe egress time（RSET）/s	Increment rate
27	0	27->26->25->24->23->22->37->42->NE3->NE2->NE1->147->156->149->150->S1	128.4	0
	60	27->28->46->SE3->SE2->SE1->148->155->152->151->150->S1	170.6	32.9%
	130	The node 27 is no longer available	——	——
93	0	93->99->98->97->96->102->NE2->NE1->147->156->149->150->S1	100.3	0
	120	93->99->98->97->96->102->NE2->NE1->147->156->149->150->S1	106.4	6.1%
	300	93->99->100->95->101->SE2->SE1->148->155->152->151->150->S1	137.2	36.8%

From Fig.14 and Fig.15, it can be seen that the equipment area of the lower deck is almost engulfed by smoke at 300s after the start of fire. The office area of the mezzanine deck is relatively less affected by smoke than the lower deck. At 60s, the route from node 24 to node 56 and the route from node 25 to node 56 are already blocked due to the spread of smoke.

From Table 6, it is known that for the equipment area (node 27 as shown in Fig.11), the optimal evacuation route is changed from NE stairway to SE stairway at 60s after the start of fire. For the muster station S1, the optimal route becomes 27-28-46-SE3-SE2-SE1-148-155-152-151-150-S1 and the RSET increases to 170.6s due to the influence of smoke. At 130s after fire occurs, the smoke has spread to node 27 and all the route through the node 27 is unavailable. Therefore, it is recommended that the evacuees on the equipment area of the lower deck should evacuate before 130s. The office area of the mezzanine deck is affected by smoke around 120s. The RSET increases by 6.1%. With the further spread of the smoke, the optimal evacuation route from node 93 to the muster station S1 is changed to 93-99-100-95-101-SE2-SE1-148-155-152-151-150-S1 at 300s after the start of fire. The RSET increases by 36.8% considering the influence of smoke.

5. Conclusions and discussions

The traditional ACO is improved by taking into account the influence of smoke temperature, visibility and CO concentration on evacuation. The dynamic optimisation model of the evacuation route is proposed by incorporating the real-time propagation of smoke on drilling platforms. The purpose is studying the visualization of the influence of smoke on evacuation. It can be tailored to cope with evaluations due to fires in other structures.

The proposed route optimisation algorithm is tested and configured to visualize and optimize the evacuation route of an illustrative offshore drilling platform. The case study shows that the route optimisation algorithm can be used to adjust the evacuation plan according to the real-time propagation of smoke. Therefore, the generic model can be used to aid real-time evacuation decisions in fire scenarios. From the case study, the real implications are that when the pool fire occurs around the oil pipeline at the lower deck, the equipment area of the lower deck is mostly affected by smoke. The office area of the mezzanine deck is relatively less affected at the beginning, but the RSET increases due to the influence of smoke.

FDS simulation of different fire scenarios has been carried out before fire accidents to build a database of the offshore drilling platform fire. Once a fire occurs, the fire simulation data of similar scenarios is selected to be analysed to determine the optimal evacuation route using the proposed dynamic route optimization model in this paper. It will provide the optimal route as fast as possible for decision makers to dynamically adjust the emergency evacuation plan and guide the evacuees to evacuate as soon as possible.

There are also some limitations in the current research. Firstly, the approach did not consider the different speeds at which evacuees walk while going up the stairs, down the stairs or at a horizontal level. Secondly, the total evacuation time including the response time has not been investigated. Thirdly, the approach did not take into account the congestion along the evacuation routes. The above problems will be further studied to characterize the influence of fire on evacuation behaviour and analyse the total evacuation time for all evacuees to assess the fire risk. The accuracy of the optimization results for emergency evacuation under fire scenarios will be improved further.

Acknowledgements

This work is supported by Research Project of “National Natural Science Foundation of China (Grant no. 52171353)”, "Special Fund for the Technology-Benefiting-People Program in Qingdao" (No.21-1-4-sf-3-nsh) and “Shandong Provincial Natural Science Foundation” (No. ZR2019MEE080). This research has received funding from the European Union’s Horizon 2020 research and innovation program under the Marie Skłodowska-Curie grant agreement H2020-MSCA-IF-2018-840425.

References

[1] Zhang J J, Zhao J C, Song Z S, GAO J. Evacuation performance of participants in an offshore platform under smoke situations. Ocean Engineering. 2020; 216:107739.

[2] Skogdalen J E, Khorsandi J, Vinnem J E. Evacuation, escape, and rescue experiences from offshore accidents including the Deepwater Horizon. Journal of Loss Prevention in the Process Industry. 2012; 25:148-158.

[3] Norazahar N, Khan F, Veith B, MacKinnon S. Dynamic risk assessment of escape and evacuation on offshore installations in a harsh environment. Applied Ocean Resarch. 2018; 79:1-6.
[4] Norazahar N, Khan F, Veith B, MacKinnon S. Prioritizing safety critical human and organizational factors of EER systems of offshore installations in a harsh environment. Safety Science. 2017; 95:171-181.
[5] Norazahar N, Smith J, Khan F, Veith B. The use of a virtual environment in managing risks associated with human responses in emergency situations on offshore installations. Ocean Engineering. 2018; 147:621-628.[6] LI J J, CHEN G M, ZHU Y. Coupling risk of fire evacuation for offshore oil and gas platforms. Acta Petrolei Sinica. 2016;37(12):1557-1562.
[7] Ping P, Wang K, Kong D P. Analysis of emergency evacuation in an offshore platform using evacuation simulation modeling. Physica A. 2018;505:601-612.
[8] Cheng J C P, Tan Y, Song Y Z, Mei Z Y, Gan V J L, WANG X Y. Developing an evacuation evaluation model for offshore oil and gas platforms using BIM and agent-based model. Automation in Construction. 2018;89:214-224.
[9] Gai W M, Deng Y F, Jiang Z A, Li J, Du Y. Multi-objective evacuation routing optimisation for toxic cloud releases. Reliability Engineering & System Safety. 2017;159:58-68.
[10] Bi C K, Pan G S, Yang L, Lin C C, Hou M, Huang Y Q. Evacuation route recommendation using auto-encoder and Markov decision process. Applied Soft Computing. 2019;84:105741.
[11] Wu C L, Chau K W. Prediction of rainfall time series using modular soft computing methods[J]. Engineering Applications of Artificial Intelligence, 2013, 26(3):997-1007.[12] Taormina R, Chau K W. ANN-based interval forecasting of streamflow discharges using the LUBE method and MOFIPS[J]. Engineering Applications of Artificial Intelligence, 2015, 45:429-440.
[13] Shamshirband S, Rabczuk T, Chau K W. A Survey of Deep Learning Techniques: Application in Wind and Solar Energy Resources[J]. IEEE Access, 2019, 7:164650-164666.
[14] Sun Q, Turkan Y. A BIM-based simulation framework for fire safety management and investigation of the critical factors affecting human evacuation performance. Advanced Engineering Informatics. 2020;44:101093.
[15] Wahlqvist J, van Hees P. Validation of FDS for large-scale well-confined mechanically ventilated fire scenarios with emphasis on predicting ventilation system behavior. Fire Safety Journal. 2013;62:102-114.
[16] Zhao D, Jiang J C, Zhou R, Tong Y, Wu F, Shi L J. Numerical study on the optimisation of smoke ventilation mode for interchange subway station fire. International Journal of Ventilation. 2016;15:79-93.
[17] Harish R, Venkatasubbaiah K. Numerical study of water spray interaction with fire plume in dual chambers connected to tall shaft. Fire Safety Journal. 2015;74:1-10.
[18] Li Q, Fang Z, Yuan J-p, Tang Z. Numerical Simulation on Impacts of Longitudinal Ventilation on Tunnel Fire Detection. Procedia Engineering. 2016;135:275-280.
[19] Lei W J, Tai C M. Effect of different staircase and exit layouts on occupant evacuation. Safety Science. 2019;118:258-263.
[20] Wang L, Zeng J, Ren C X. Research on evacuation ability of student dormitory building fire in certain university based on FDS + EVAC. Journal of Safety Science and Technology. 2018;14:136-142.
[21] Grimaz S, Tosolini E. Application of rapid method for checking egress system vulnerability. Fire Safety Journal. 2013;58:92-102.
[22] Lovreglio R, Ronchi E, Borri D. The validation of evacuation simulation models through the

analysis of behavioural uncertainty. Reliability Engineering & System Safety. 2014;131:166-174.
[23] Zhuang Y Z, Ding H, Zheng G P, Cui Y K, Huang Y. Study on Ventilation System Linkage Control Strategy in a Double-Hole Tunnel Fire. Advances in Materials Science and Engineering. 2020;5:1-14
[24] Wang S H, Wang W C, Wang K C, Shih SY. Applying building information modeling to support fire safety management. Automation in Construction. 2015;59:158-167.
[25] Shi J, Dao J, Jiang L, Pan Z. Research on IFC- and FDS-Based Information Sharing for Building Fire Safety Analysis. Advances in Civil Engineering. 2019;2019:3604369.
[26] Alonso-Gutierrez V, Cuesta A, Alvear D, Lazaro M. The Impact of a Change on the Size of the Smoke Compartment in the Evacuation of Health Care Facilities. Fire Technology. 2018;54:335-354.
[27] Krol A, Krol M. The factors determining the number of the endangered people in a case of fire in a road tunnel. Fire Safety Journal. 2020;111:102942.
[28] Chiu C W, Chen C H, Chen J C, Shu C M. Analyses of smoke management models in TFT-LCD cleanroom. Building Simulation. 2013;6:403-413.
[29] Yi W, Kumar A. Ant colony optimisation for disaster relief operations. Transportation Research Part E: Logistics and Transportation Review. 2007;43:660-672.
[30] Fang Z X, Zong X L, Li Q Q, Li Q P, Xiong S W. Hierarchical multi-objective evacuation routing in stadium using ant colony optimisation approach. Journal of Transport Geography. 2011;19:443-451.
[31] Yang X X, Dong H R, Yao X M. Passenger distribution modelling at the subway platform based on ant colony optimisation algorithm. Simulation Modelling Practice and Theory. 2017;77:228-244.
[32] Kevin McGrattan, Simo Hostikka, Randall McDermott, et al., Fire Dynamics Simulator User's Guide (Sixth Edition),NIST & VTT,2013.
[33] Stroup D, Lindeman A, Verification and Validation of Selected Fire Models for Nuclear Power Plant Applications, NUREG-1824, Supplement 1, United States Nuclear Regulatory Commission, Washington, DC, 2013.
[34] Guide for Determining the Fire Endurance of Concrete Elements[M], ACI-216-89, American Concerete Institute, Detroit, 1989.
[35] Hurley M J , Gottuk D T , Hall J R , et al. SFPE handbook of fire protection engineering, fifth edition[M], Massachusetts: National Fire Protection Association, 2016.
[36] Elhelw M , El-Shobaky A , Attia A , et al. Advanced dynamic modeling study of fire and smoke of crude oil storage tanks[J]. Process Safety and Environmental Protection, 2021, 146(B3):670-685.
[37] Halim S Z, Janardanan S, Flechas T, Mannan M S. In search of causes behind offshore incidents: Fire in offshore oil and gas facilities. Journal of Loss Prevention in the Process Industry. 2018;54:254-265.
[38] Adjiski V, Mirakovski D, Despodov Z, Mijalkovski S. Simulation and optimisation of evacuation routes in case of fire in underground mines. Journal of Sustainable Mining. 2015;14:133-143.
[39] Milke J A. Evaluating the Early Development of Smoke Hazard from Fires in Large Spaces. Transactions-American Society of Heating Refrigerating and Air Conditioning Engineers. 2000;106:627-636.
[40] Roh J S, Ryou H S, Park W H, Jang Y J. CFD simulation and assessment of life safety in a subway train fire. Tunnelling and Underground Space Technology. 2009;24:447-453.
[41] Tsukahara M, Koshiba Y, Ohtani H. Effectiveness of downward evacuation in a large-scale subway fire using Fire Dynamics Simulator. Tunnelling and Underground Space Technology. 2011;26:573-581.
[42] Yi S-L. Performance-based Fire Smoke Virtual Reality Simulation and Analysis of Exchanging Subway Station. Journal of System Simulation. 2013;25:681-686.

[43] Baeza D, Ihle C F, Ortiz J M. A comparison between ACO and Dijkstra algorithms for optimal ore concentrate pipeline routing. Journal of Cleaner Production. 2017;144:149-160.
[44] Fang Z X, Zong X L, Li Q Q, Li Q P, Xiong S W. Hierarchical multi-objective evacuation routing in stadium using ant colony optimisation approach. Journal of Transport Geography. 2011;19:443-451.
[45] Jin T, Yamada T. Irritating Effects of Fire Smoke on Visibility. Fire Science and Technology. 1985;5:79-90.
[46] Qiao Y F, WU J Z. A Study on the Impacts of the Fire Product at Subway Stations on Evacuation Speeds of Pedestrians. Journal of Transportation Engineering and Information. 2017;15:128-133.58
[47] Dorigo M, Maniezzo V, Colorni A. Ant system: optimisation by a colony of cooperating agents. IEEE Transactions on Systems Man & Cybernetics. 1996;26:29-41.
[48] Gao S C, Wang Y R, Cheng J J, Yasuhiro I, Zheng T. Ant colony optimisation with clustering for solving the dynamic location routing problem. Applied Mathematics and Computation. 2016;285:149-173.